Hindawi
Mathematical Problems in Engineering
Volume 2017, Article ID 5830279, 9 pages
https://doi.org/10.1155/2017/5830279

Research Article

CuO–Water Nanofluid Magnetohydrodynamic Natural Convection inside a Sinusoidal Annulus in Presence of Melting Heat Transfer

M. Sheikholeslami,[1] R. Ellahi,[2] and C. Fetecau[3]

[1] *Department of Mechanical Engineering, Babol Noshirvani University of Technology, Babol, Iran*
[2] *Department of Mathematics & Statistics, FBAS, IIUI, H-10 Sector, Islamabad, Pakistan*
[3] *Academy of Romanian Scientists, 050094 Bucharest, Romania*

Correspondence should be addressed to R. Ellahi; rahmatellahi@yahoo.com

Received 23 April 2017; Accepted 3 July 2017; Published 31 July 2017

Academic Editor: Efstratios Tzirtzilakis

Impact of nanofluid natural convection due to magnetic field in existence of melting heat transfer is simulated using CVFEM in this research. KKL model is taken into account to obtain properties of CuO–H_2O nanofluid. Roles of melting parameter (δ), CuO–H_2O volume fraction (ϕ), Hartmann number (Ha), and Rayleigh (Ra) number are depicted in outputs. Results depict that temperature gradient improves with rise of Rayleigh number and melting parameter. Nusselt number detracts with rise of Ha. At the end, a comparison as a limiting case of the considered problem with the existing studies is made and found in good agreement.

1. Introduction

Melting process has various uses such as application like in thermocouple, heat exchangers, and heat engines. Chamkha and Ismael [1] examined the Cu-H2O nanofluid mixed convection in an enclosure with lid wall. Also, Ellahi et al. [2] reported the similar study for nanofluid over permeable wedge in mixed convection. Harikrishnan et al. [3] investigated melting behavior of composite PCM for heating application. Nanofluid melting in a pipe with external fins has been studied by Mat et al. [4]. Manikandan and Rajan [5] utilized hybrid nanofluid for heat transfer augmentation. Koca et al. [6] utilized Ag-H2O nanofluid for natural circulation loops. Shyam and Tiwari [7] investigated the coiled heat exchanger by means of nanofluid. Das [8] reported the radiative flow in existence of melting heat.

Sheremet et al. [9] illustrated the free convective flow of ferrofluid in a rotating enclosure. Wavy duct in existence of Brownian forces has been examined by Shehzad et al. [10]. Sheikholeslami et al. [11] illustrated different uses of nanotechnology in their article paper. Abbas et al. [12] demonstrated the nanofluid flow through a horizontal Riga plate. Chamkha and Rashad [13] reported the nanoparticle migration on porous cone. Ellahi et al. [14] analyzed particle shape effects on Marangoni convection boundary layer flow of a nanofluid. They considered the Lorentz forces impact in governing equations. Malvandi et al. [15] reported nanofluid flow inside a channel in existence of Lorentz forces. Garoosi et al. [16] investigated performance of heat exchanger via nanofluid. They indicated that optimum volume fraction of nanoparticle exists to obtain maximum Nusselt number. Mesoscopic method has been utilized by Sheikholeslami and Ellahi [17] for a three-dimensional problem.

This research intends to present the impact of melting heat transfer on free convection of ferrofluid in the presence of Lorentz forces. CVFEM is selected to find the outputs. Roles of melting parameter, CuO–water volume fraction, and Hartmann and Rayleigh numbers are presented.

2. Problem Statement

Figure 1 depicts the geometry, boundary condition, and sample element. The inner wall is hot wall ($T = T_h$) and

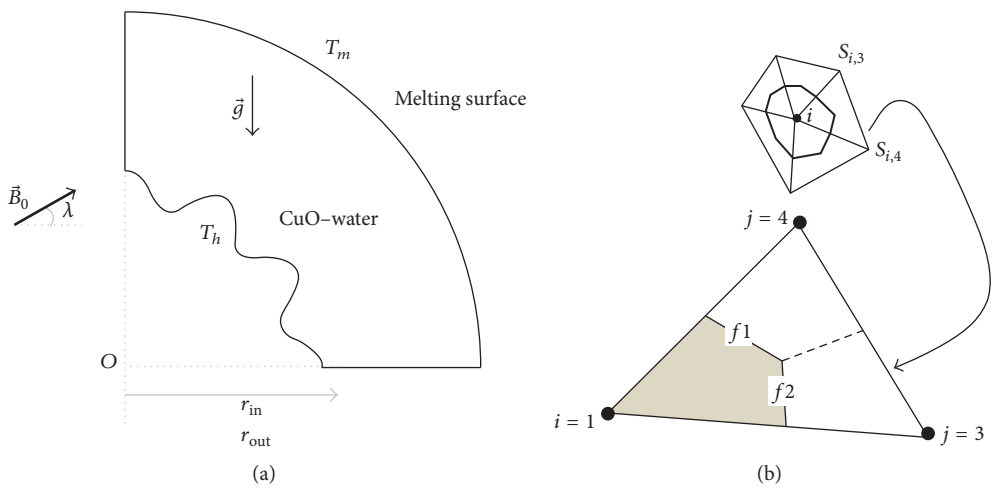

Figure 1: (a) Geometry; (b) sample element.

the outer one is melting surface ($T = T_m$). Other walls are adiabatic. Horizontal magnetic field has been applied. The enclosure is field with nanofluid.

3. Governing Equation and Simulation

3.1. Governing Formulation. 2D steady convective nanofluid flow is considered in existence of constant magnetic field. The fluid flow is laminar and incompressible. The flow is steady and Newtonian. The viscous dissipation is negligible in this study. The effects of Brownian force and thermophoretic force are not taken into condition. The flow also follows the Boussinesq assumption. The prevailing equations under these constraints can be written as [20]

$$\begin{aligned}
&\frac{\partial v}{\partial y} + \frac{\partial u}{\partial x} = 0,\\
&(\rho_{\mathrm{nf}})\left(v\frac{\partial u}{\partial y} + u\frac{\partial u}{\partial x}\right)\\
&\quad = \left[B_y\sigma_{\mathrm{nf}}vB_x - B_y^2\sigma_{\mathrm{nf}}u + \mu_{\mathrm{nf}}\left(\frac{\partial^2 u}{\partial y^2} + \frac{\partial^2 u}{\partial x^2}\right) - \frac{\partial P}{\partial x}\right].\\
&\rho_{\mathrm{nf}}\left(\frac{\partial v}{\partial y}v + \frac{\partial v}{\partial x}u\right)\\
&\quad = uB_y\sigma_{\mathrm{nf}}B_x + (T - T_c)\beta_{\mathrm{nf}}g\rho_{\mathrm{nf}} - vB_x\sigma_{\mathrm{nf}}B_x\\
&\qquad + \left(\frac{\partial^2 v}{\partial x^2} + \frac{\partial^2 v}{\partial y^2}\right)\mu_{\mathrm{nf}} - \frac{\partial P}{\partial y},\\
&B_x = B_o\cos\lambda,\\
&B_y = B_o\sin\lambda,\\
&(\rho C_p)_{\mathrm{nf}}\left(v\frac{\partial T}{\partial y} + u\frac{\partial T}{\partial x}\right) = k_{\mathrm{nf}}\left(\frac{\partial^2 T}{\partial x^2} + \frac{\partial^2 T}{\partial y^2}\right),
\end{aligned} \tag{1}$$

$(\rho C_p)_{\mathrm{nf}}$, ρ_{nf}, $(\rho\beta)_{\mathrm{nf}}$, and σ_{nf} are calculated as [17, 18]

$$\begin{aligned}
&(\rho C_p)_{\mathrm{nf}} = \phi(\rho C_p)_s + (1-\phi)(\rho C_p)_f,\\
&\rho_{\mathrm{nf}} = \rho_f(1-\phi) + \phi\rho_s,\\
&(\rho\beta)_{\mathrm{nf}} = \phi(\rho\beta)_s + (1-\phi)(\rho\beta)_f,\\
&\sigma_{\mathrm{nf}}\\
&\quad = \sigma_f\left[\left(\frac{+(2+\sigma_s/\sigma_f) - \phi(-1+\sigma_s/\sigma_f)}{3\phi(-1+\sigma_s/\sigma_f)}\right)^{-1} + 1\right].
\end{aligned} \tag{2}$$

k_{nf}, μ_{nf} are calculated via KKL model [19]:

$$\begin{aligned}
&\frac{k_{\mathrm{nf}}}{k_f} = 1 + \frac{3(k_p/k_f - 1)\phi}{(k_p/k_f + 2) - (k_p/k_f - 1)\phi} + 5\\
&\quad \times 10^4 g'(\phi, T, d_p)\phi\rho_f c_{p,f}\sqrt{\frac{\kappa_b T}{d_p\rho_p}},\\
&R_f = 4\times 10^{-8}\,\mathrm{km^2/W},\\
&R_f = -d_p(1/k_p - 1/k_{p,\mathrm{eff}}),\\
&g'(\phi, d_p, T) = \ln(T)\left(a_1 + a_3\ln(\phi) + a_2\ln(d_p)\right.\\
&\quad \left. + a_5\ln(d_p)^2 + a_4\ln(d_p)\ln(\phi)\right) + \left(a_6 + a_8\ln(\phi)\right.\\
&\quad \left. + a_7\ln(d_p) + a_{10}\ln(d_p)^2 + a_9\ln(\phi)\ln(d_p)\right),\\
&\mu_{\mathrm{nf}} = \frac{\mu_f}{(1-\phi)^{2.5}} + \frac{k_{\mathrm{Brownian}}}{k_f}\times\frac{\mu_f}{\mathrm{Pr}}.
\end{aligned} \tag{3}$$

Properties and needed parameters are provided in Tables 1 and 2 [19].

Table 1: Coefficient values of CuO–H_2O [19].

Coefficient values	CuO–water
a_1	−26.5933108
a_2	−0.403818333
a_3	−33.3516805
a_4	−1.915825591
a_5	$6.421858E-02$
a_6	48.40336955
a_7	−9.787756683
a_8	190.245610009
a_9	10.9285386565
a_{10}	−0.72009983664

Vorticity and stream function should be used to eliminate pressure source terms:

$$\omega + \frac{\partial u}{\partial y} - \frac{\partial v}{\partial x} = 0, \quad \frac{\partial \psi}{\partial x} = -v, \quad \frac{\partial \psi}{\partial y} = u. \tag{4}$$

Dimensionless quantities are introduced as follows:

$$P = \frac{p}{\rho_{\mathrm{nf}} \left(\alpha_{\mathrm{nf}}/L\right)^2}, \quad U = \frac{uL}{\alpha_{\mathrm{nf}}}, \quad V = \frac{vL}{\alpha_{\mathrm{nf}}}, \quad \theta = \frac{T - T_m}{T_h - T_m}, \quad (X, Y) = \frac{(x, y)}{L}, \quad \Psi = \frac{\psi}{\alpha_{\mathrm{nf}}}, \quad \Omega = \frac{\omega L^2}{\alpha_{\mathrm{nf}}}. \tag{5}$$

The final formulae are

$$\Omega + \frac{\partial^2 \Psi}{\partial Y^2} + \frac{\partial^2 \Psi}{\partial X^2} = 0,$$

$$\frac{\partial \Omega}{\partial X} U + V \frac{\partial \Omega}{\partial Y} = \mathrm{Pr} \frac{A_5}{A_1} \frac{A_2}{A_4} \left(\frac{\partial^2 \Omega}{\partial Y^2} + \frac{\partial^2 \Omega}{\partial X^2} \right) + \mathrm{PrHa}^2 \cdot \frac{A_6}{A_1} \frac{A_2}{A_4} \left(-\frac{\partial V}{\partial X} B_x B_x + B_y \frac{\partial U}{\partial X} B_x - \frac{\partial V}{\partial Y} B_y B_x + B_y \frac{\partial U}{\partial Y} B_y \right) + \mathrm{PrRa} \frac{A_3 A_2^2}{A_1 A_4^2} \frac{\partial \theta}{\partial X},$$

$$\frac{\partial \theta}{\partial X} U + \frac{\partial \theta}{\partial Y} V = \left(\frac{\partial^2 \theta}{\partial X^2} + \frac{\partial^2 \theta}{\partial Y^2} \right). \tag{6}$$

Boundary conditions are

$$\frac{\partial \theta}{\partial n} = 0.0 \quad \text{on other walls}, \quad \theta = 0 \quad \text{on outer wall}, \quad \theta = 1.0 \quad \text{on inner wall}, \quad \Psi = 0.0 \quad \text{on all walls except melting surface} \tag{7}$$

and in melting surface, we have

$$\frac{\partial \theta}{\partial n} = \frac{A_2}{A_1} \frac{1}{\delta} \left(L + c_s \left(T_m - T_0 \right) \right) \frac{\partial \Psi}{\partial n}, \tag{8}$$

where dimensionless and constants parameters are illustrated as

$$\mathrm{Pr} = \frac{\upsilon_f}{\alpha_f}, \quad \mathrm{Ra} = \frac{g \beta_f \Delta T L^3}{\left(\upsilon_f \alpha_f\right)}, \quad \mathrm{Ha} = L B_0 \sqrt{\frac{\sigma_f}{\mu_f}}, \quad \delta = \frac{\left(\rho C_p\right)_f}{\rho_f} \frac{\left(T_h - T_m\right)}{1 + c_s \left(T_m - T_0\right)}, \quad A_1 = \frac{\rho_{\mathrm{nf}}}{\rho_f}, \quad A_5 = \frac{\mu_{\mathrm{nf}}}{\mu_f}, \quad A_2 = \frac{\left(\rho C_P\right)_{\mathrm{nf}}}{\left(\rho C_P\right)_f}, \quad A_6 = \frac{\sigma_{\mathrm{nf}}}{\sigma_f}, \quad A_4 = \frac{k_{\mathrm{nf}}}{k_f}, \quad A_3 = \frac{(\rho \beta)_{\mathrm{nf}}}{(\rho \beta)_f}. \tag{9}$$

It should be mentioned that δ is related to Stefan numbers.

Local and average Nusselt over the cold wall can be calculated as follows:

$$\mathrm{Nu}_{\mathrm{loc}} = \left(\frac{k_{\mathrm{nf}}}{k_f} \right) \frac{\partial \theta}{\partial r}, \quad \mathrm{Nu}_{\mathrm{ave}} = \frac{1}{0.5\pi} \int_0^{0.5\pi} \mathrm{Nu}_{\mathrm{loc}} \, d\xi. \tag{10}$$

Table 2: Properties of H_2O and CuO [19].

	ρ (kg/m^3)	C_p (j/kgk)	k (W/m·k)	$\beta \times 10^5$ (K^{-1})	d_p (nm)	σ $(\Omega \cdot \mathrm{m})^{-1}$
Water	997.1	4179	0.613	21	—	0.05
CuO	6500	540	18	29	45	10^{-10}

Table 3: Mesh independency analysis when Ra = 10000, $\delta = 0.2$, Ha = 40, and $\phi = 0.04$.

Mesh size	51×151	61×181	71×211	81×241	91×271
$\mathrm{Nu}_{\mathrm{ave}}$	0.890241	0.895531	0.907145	0.908743	0.909166

Table 4: $\mathrm{Nu}_{\mathrm{ave}}$ for various Gr and Ha at Pr = 0.733.

Ha	Gr = 2×10^4		Gr = 2×10^5	
	Present work	Rudraiah et al. [20]	Present work	Rudraiah et al. [20]
0	2.5665	2.5188	5.093205	4.9198
10	2.26626	2.2234	4.9047	4.8053
50	1.09954	1.0856	2.67911	2.8442
100	1.02218	1.011	1.46048	1.4317

3.2. Numerical Procedure. CVFEM uses both benefits of two common CFD methods. This method uses triangular element (see Figure 1(b)). Upwind approach is utilized for advection term. Gauss-Seidel approach is applied to solve the algebraic equations. Further notes can be found in [21].

4. Grid Independency and Validation

Outputs should not rely on mesh size. Therefore, several grids should be tested. For example, as shown in Table 3, a grid size of 71×211 can be selected. The correctness of CVFEM code for nanofluid natural convective heat transfer is demonstrated in Figure 2 ([18]). This CVFEM code has good accuracy for magnetohydrodynamic flow as depicted in Table 4 [20].

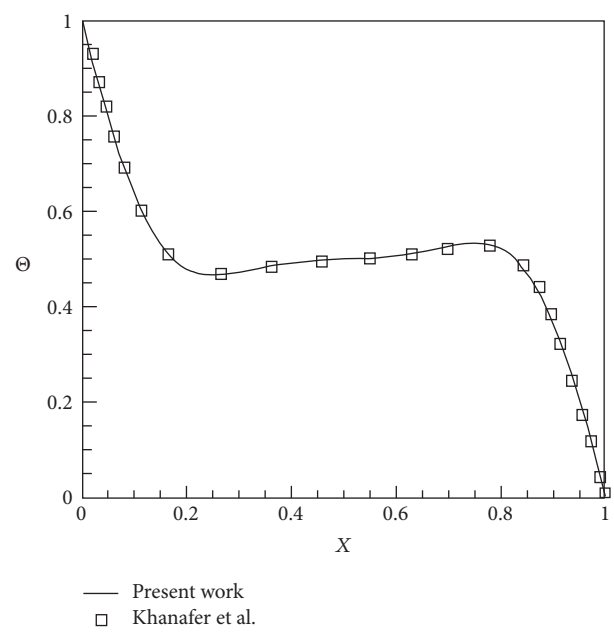

Figure 2: Validation of present code (Khanafer et al. [18]) when Gr = 10^4, $\phi = 0.1$, and Pr = 6.8 (Cu–water).

5. Results and Discussion

Nanofluid flow in a half sinusoidal annulus due to magnetic field in presence of melting surface is examined. μ_{nf}, k_{nf} of CuO–water nanofluid are estimated by means of KKL model. Graphs and tables are depicted for different amounts of CuO–H_2O volume fraction (ϕ = 0 to 0.04), melting parameter (δ = 0 to 0.2), Rayleigh number (Ra = 500 to 5000), and Hartmann number (Ha = 0 to 40).

Impact of adding CuO nanoparticles in water on velocity and temperature contours is depicted in Figure 3. Temperature gradient decreases with augment of ϕ. $|\Psi_{\max}|$ augments with adding nanoparticles because of increment in the solid movements. In presence of melting heat transfer and magnetic field, effect of adding nanoparticles on isotherms becomes negligible.

Figures 4 and 5 depict the impact of Rayleigh and Hartmann numbers in absence of melting heat transfer. There is only one eddy in streamline. In low Rayleigh number, conduction mechanism is dominant. As Ra increases, the distortion of isotherms is enhanced close to the hot wall. Adding magnetic field makes isotherms become parallel. In presence of melting heat transfer the primary eddy diminishes and increasing Lorentz forces generates three layers for streamline. Increasing melting parameter augments the bottom eddy.

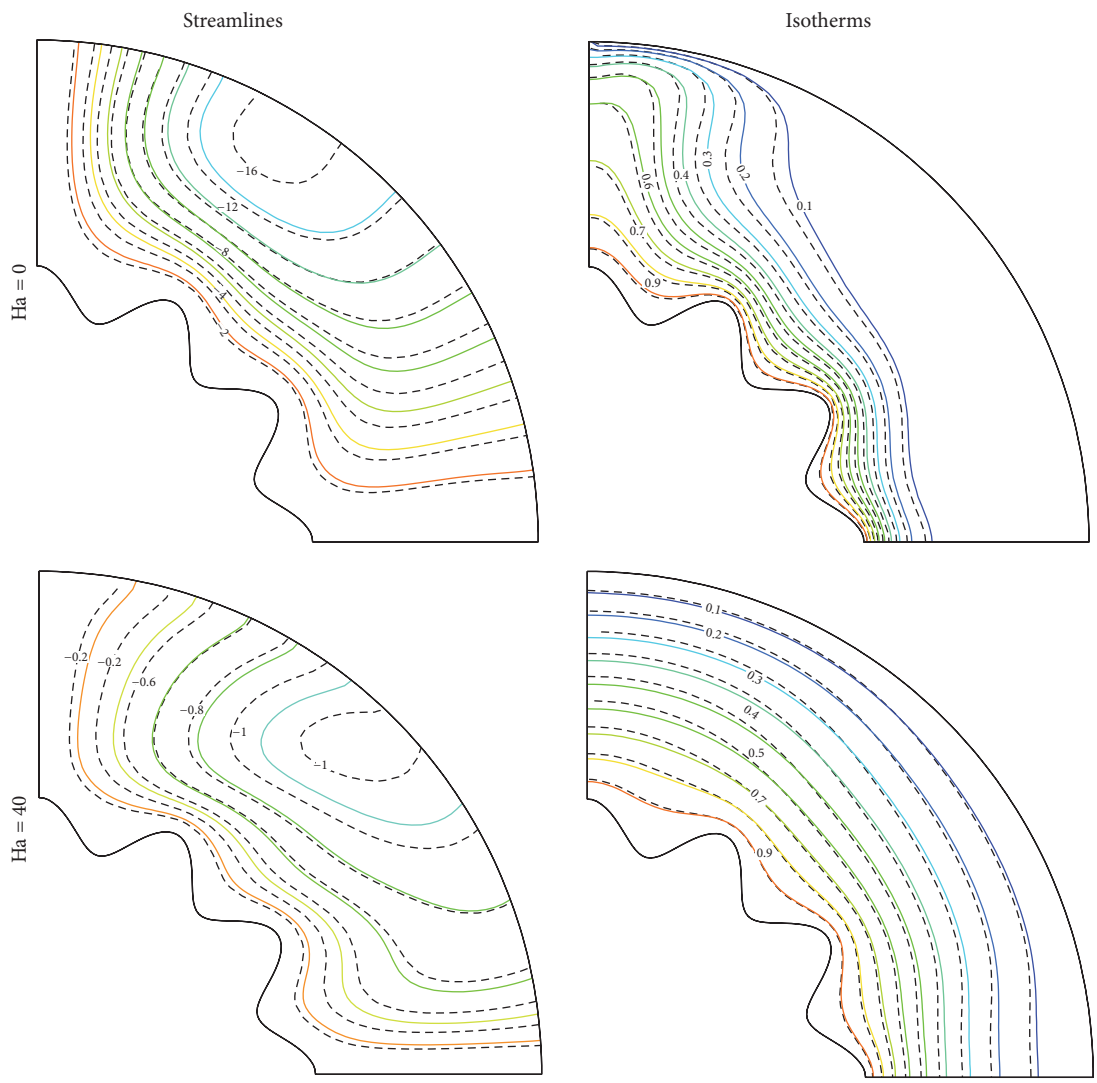

FIGURE 3: Impact of adding CuO in water on streamlines and isotherms (nanofluid ($\phi = 0.04$) (—) and pure fluid ($\phi = 0$) (- - -)) when Ra = 5000 and $\delta = 0.2$.

Figure 6 illustrates the impact of δ, Ra, and Ha on $\mathrm{Nu}_{\mathrm{ave}}$. The formula for $\mathrm{Nu}_{\mathrm{ave}}$ corresponding to active parameters is

$$\begin{aligned}\mathrm{Nu}_{\mathrm{ave}} &= 0.799 + 0.305\delta + 0.19\mathrm{Ra}^* - 0.16\mathrm{Ha}^* \\ &\quad + 0.003\mathrm{Ra}^*\delta - 0.0039\delta\mathrm{Ha}^* - 0.028\mathrm{Ra}^*\mathrm{Ha}^* \\ &\quad + 0.058\delta^2 - 0.012\mathrm{Ra}^{*2} + 0.039\mathrm{Ha}^{*2},\end{aligned} \tag{11}$$

where $\mathrm{Ha}^* = 0.1\mathrm{Ha}$ and $\mathrm{Ra}^* = 0.001\mathrm{Ra}$. As melting parameter augments, temperature gradient is enhanced and in turn Nusselt number is enhanced. Increasing buoyancy forces leads the thermal boundary layer thickness to reduce. So Nusselt number increases with enhancement of Ra. As Hartmann number augments, isotherms become parallel. Therefore Nusselt number has opposite relationship with Ha.

6. Conclusions

Nanofluid free convection due to Lorentz force in existence of melting surface is reported. Combination of FEM and FVM is utilized to solve the PDEs. KKL model is considered for nanofluid. Roles of Hartmann number, CuO–water volume fraction, Rayleigh number, and melting parameter are presented. Outputs depict that temperature gradient improves with augment of melting parameter and Rayleigh number. Adding magnetic field makes the temperature gradient reduce due to domination of conduction mechanism in high Hartmann number.

Nomenclature

B: Magnetic field
T: Fluid temperature
Nu: Nusselt number

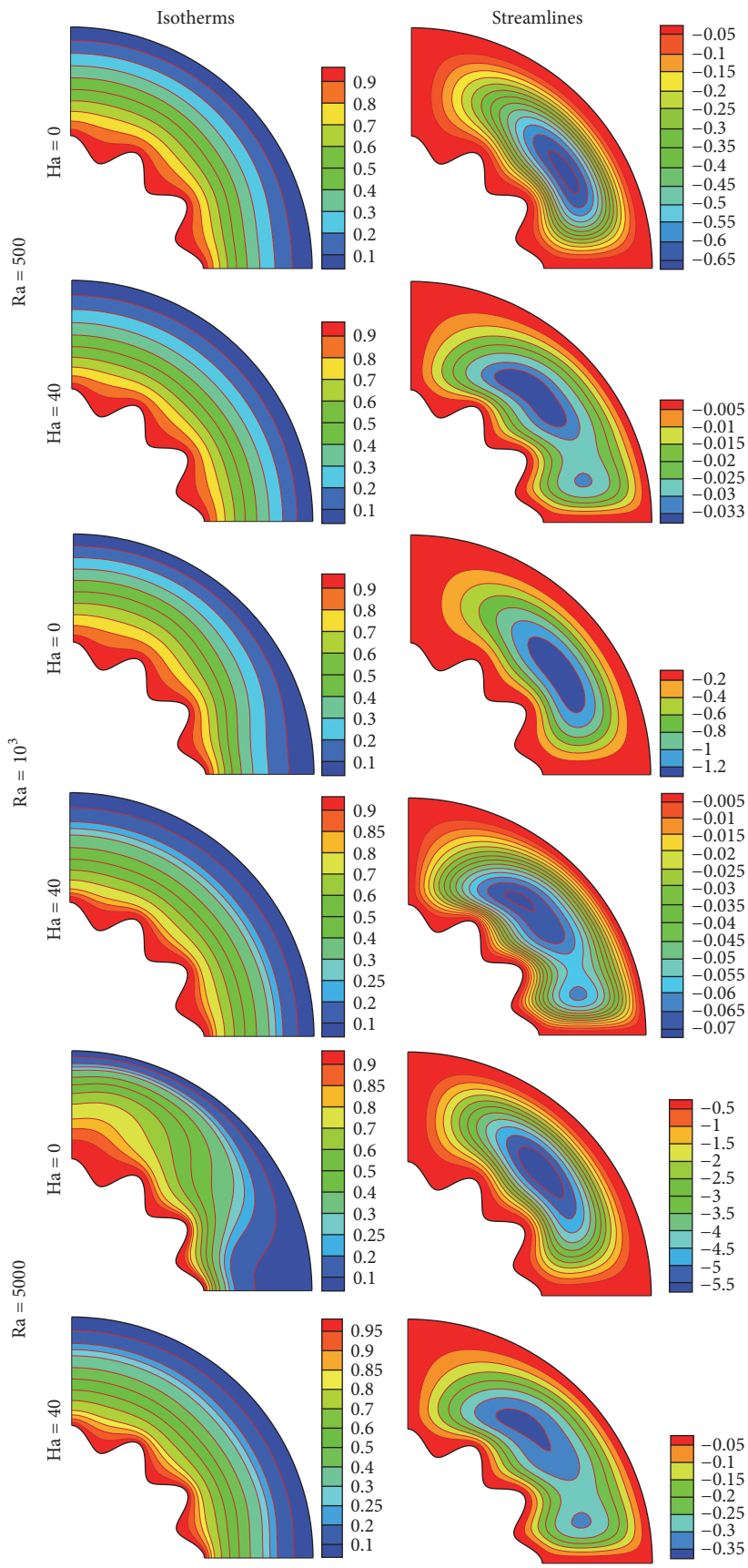

Figure 4: Isotherms and streamlines for various Ha, Ra when $\delta = 0$ and $\phi = 0.04$.

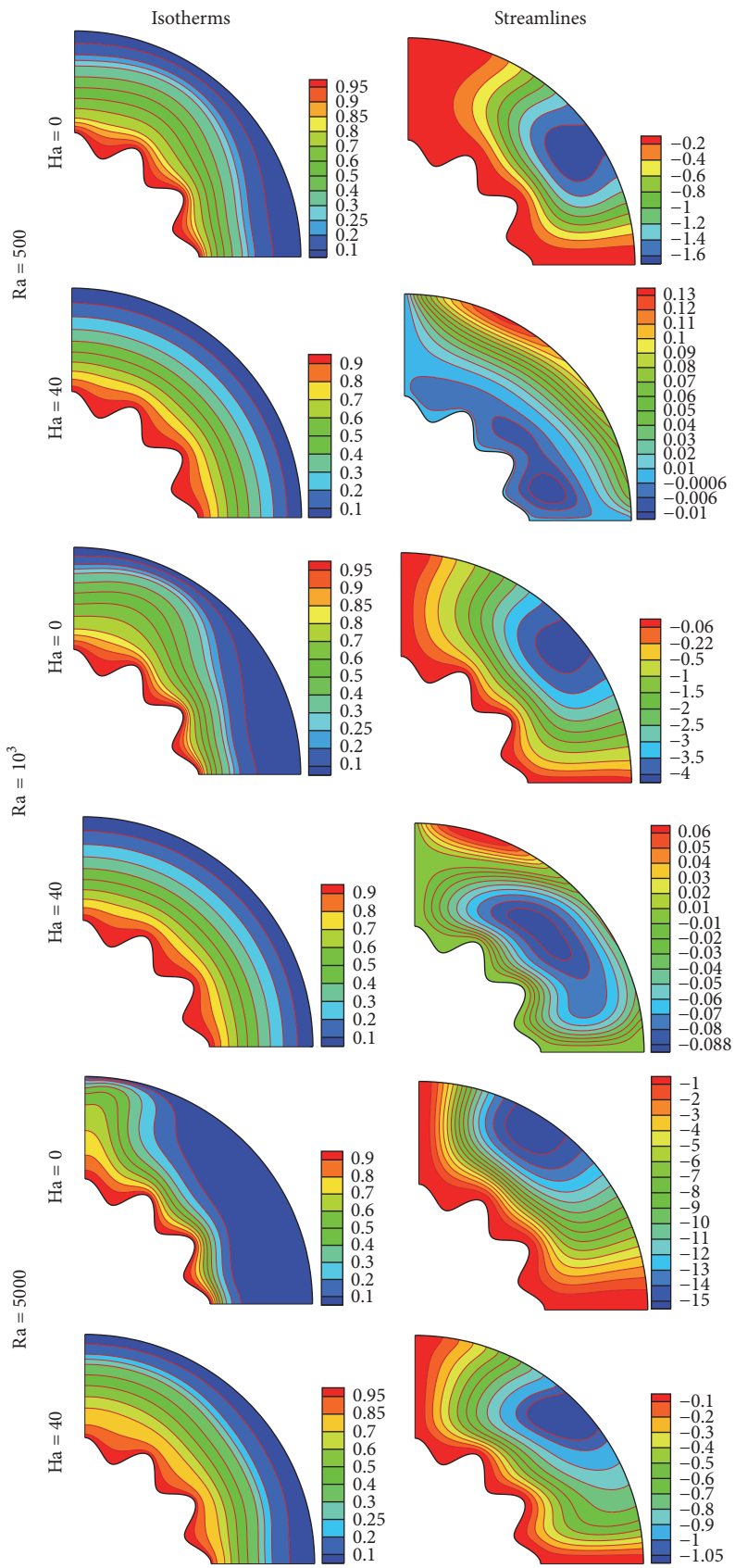

Figure 5: Isotherms and streamlines for various Ha, Ra when $\delta = 0.2$ and $\phi = 0.04$.

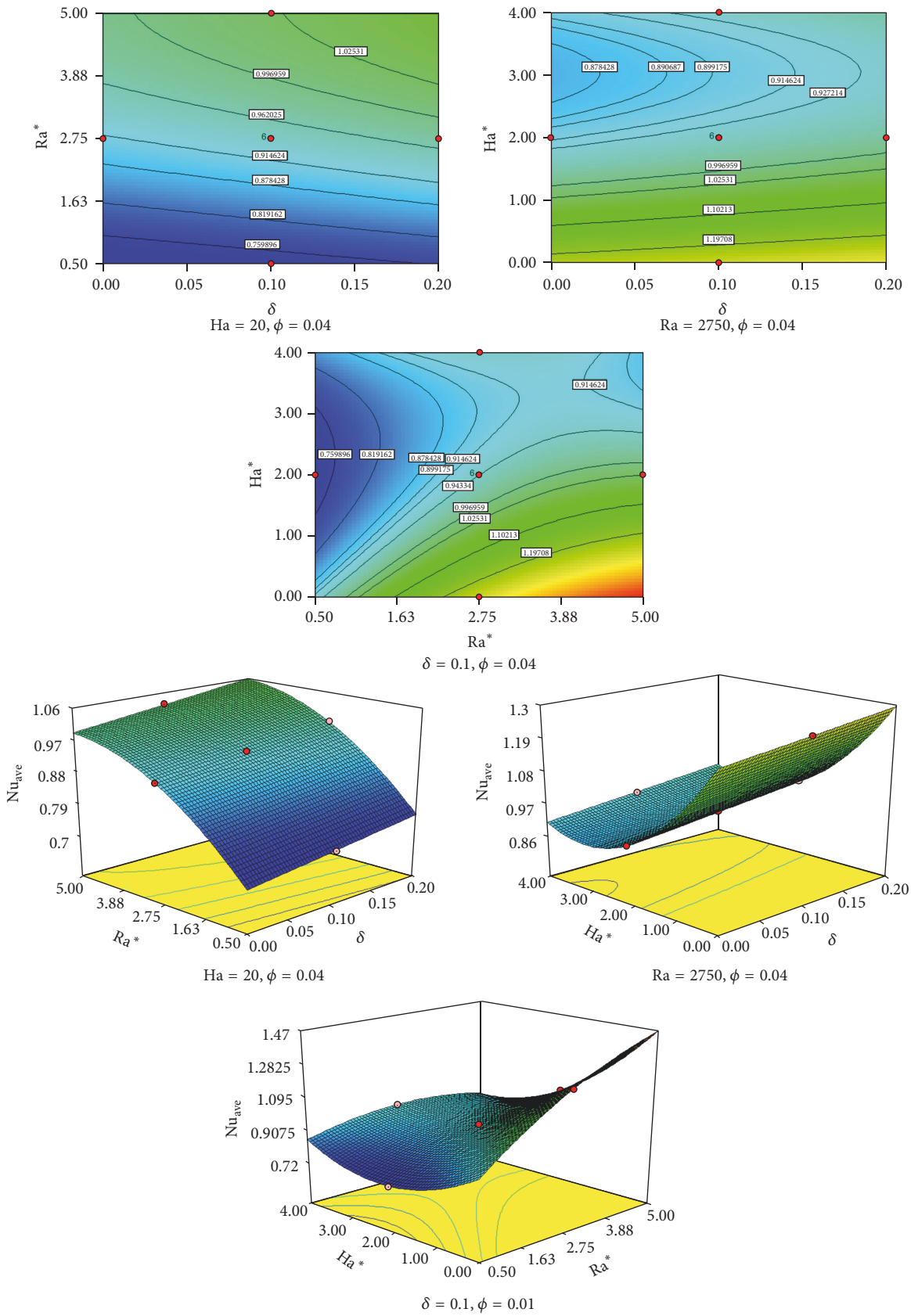

Figure 6: Impacts of δ, Ha, and Ra on Nu_{ave}.

Ra: Rayleigh number
$\vec{g}$: Gravitational acceleration vector
Ha: Hartmann number.

Greek Symbols

Θ: Dimensionless temperature
α: Thermal diffusivity
Ω and Ψ: Dimensionless vorticity and stream function
δ: Melting parameter
β: Thermal expansion coefficient
σ: Electrical conductivity
μ: Dynamic viscosity.

Subscripts

f: Base fluid
loc: Local
nf: Nanofluid.

Conflicts of Interest

The authors declare that there are no conflicts of interest regarding the publication of this paper.

References

[1] A. J. Chamkha and M. A. Ismael, "Magnetic field effect on mixed convection in lid-driven trapezoidal cavities filled with a Cu-Water nanofluid with an aiding or opposing side wall," *Journal of Thermal Science and Engineering Applications*, vol. 8, no. 3, Article ID 031009, 2016.

[2] R. Ellahi, M. Hassan, and A. Zeeshan, "Aggregation effects on water base Al2O3 - Nanofluid over permeable wedge in mixed convection," *Asia-Pacific Journal of Chemical Engineering*, vol. 11, no. 2, pp. 179–186, 2016.

[3] S. Harikrishnan, M. Deenadhayalan, and S. Kalaiselvam, "Experimental investigation of solidification and melting characteristics of composite PCMs for building heating application," *Energy Conversion and Management*, vol. 86, pp. 864–872, 2014.

[4] S. Mat, A. A. Al-Abidi, K. Sopian, M. Y. Sulaiman, and A. T. Mohammad, "Enhance heat transfer for PCM melting in triplex tube with internal-external fins," *Energy Conversion and Management*, vol. 74, pp. 223–236, 2013.

[5] S. Manikandan and K. Rajan, "New hybrid nanofluid containing encapsulated paraffin wax and sand nanoparticles in propylene glycol-water mixture: Potential heat transfer fluid for energy management," *Energy Conversion and Management*, vol. 137, pp. 74–85, 2017.

[6] H. D. Koca, S. Doganay, and A. Turgut, "Thermal characteristics and performance of Ag-water nanofluid: Application to natural circulation loops," *Energy Conversion and Management*, vol. 135, pp. 9–20, 2017.

[7] L. S. Shyam and G. N. Tiwari, "Analytical characteristic equation of nanofluid loaded active double slope solar still coupled with helically coiled heat exchanger," *Energy Conversion and Management*, vol. 135, pp. 308–326, 2017.

[8] K. Das, "Radiation and melting effects on MHD boundary layer flow over a moving surface," *Ain Shams Engineering Journal*, vol. 5, no. 4, pp. 1207–1214, 2014.

[9] M. A. Sheremet, H. F. Oztop, and I. Pop, "MHD natural convection in an inclined wavy cavity with corner heater filled with a nanofluid," *Journal of Magnetism and Magnetic Materials*, vol. 416, pp. 37–47, 2016.

[10] N. Shehzad, A. Zeeshan, R. Ellahi, and K. Vafai, "Convective heat transfer of nanofluid in a wavy channel: Buongiorno's mathematical model," *Journal of Molecular Liquids*, vol. 222, pp. 446–455, 2016.

[11] M. Sheikholeslami, Q. M. Z. Zia, and R. Ellahi, "Influence of Induced Magnetic Field on Free Convection of Nanofluid Considering Koo-Kleinstreuer-Li (KKL) Correlation," *Applied Sciences (Switzerland)*, vol. 6, no. 11, article no. 324, 2016.

[12] T. Abbas, M. Ayub, M. . Bhatti, M. M. Rashidi, and M. . Ali, "Entropy generation on nanofluid flow through a horizontal Riga plate," *Entropy. An International and Interdisciplinary Journal of Entropy and Information Studies*, vol. 18, no. 6, Paper No. 223, 11 pages, 2016.

[13] A. J. Chamkha and A. M. Rashad, "Natural convection from a vertical permeable cone in a nanofluid saturated porous media for uniform heat and nanoparticles volume fraction fluxes," *International Journal of Numerical Methods for Heat and Fluid Flow*, vol. 22, no. 8, pp. 1073–1085, 2012.

[14] R. Ellahi, A. Zeeshan, and M. Hassan, "Particle shape effects on marangoni convection boundary layer flow of a nanofluid," *International Journal of Numerical Methods for Heat and Fluid Flow*, vol. 26, no. 7, pp. 2160–2174, 2016.

[15] A. Malvandi, M. H. Kaffash, and D. D. Ganji, "Nanoparticles migration effects on magnetohydrodynamic (MHD) laminar mixed convection of alumina/water nanofluid inside microchannels," *Journal of the Taiwan Institute of Chemical Engineers*, vol. 52, pp. 40–56, 2015.

[16] F. Garoosi, F. Hoseininejad, and M. M. Rashidi, "Numerical study of natural convection heat transfer in a heat exchanger filled with nanofluids," *Energy*, vol. 109, pp. 664–678, 2016.

[17] M. Sheikholeslami and R. Ellahi, "Three dimensional mesoscopic simulation of magnetic field effect on natural convection of nanofluid," *International Journal of Heat and Mass Transfer*, vol. 89, Article ID 12118, pp. 799–808, 2015.

[18] K. Khanafer, K. Vafai, and M. Lightstone, "Buoyancy-driven heat transfer enhancement in a two-dimensional enclosure utilizing nanofluids," *International Journal of Heat and Mass Transfer*, vol. 46, no. 19, pp. 3639–3653, 2003.

[19] M. S. Kandelousi and R. Ellahi, "Simulation of ferrofluid flow for magnetic drug targeting using the lattice boltzmann method," *Zeitschrift fur Naturforschung - Section A Journal of Physical Sciences*, vol. 70, no. 2, pp. 115–124, 2015.

[20] N. Rudraiah, R. M. Barron, M. Venkatachalappa, and C. K. Subbaraya, "Effect of a magnetic field on free convection in a rectangular enclosure," *International Journal of Engineering Science*, vol. 33, no. 8, pp. 1075–1084, 1995.

[21] V. R. Voller, *Basic control volume finite element methods for fluids and solids*, vol. 1 of *IISc Research Monographs Series*, World Scientific Publishing Co. Pte. Ltd., Hackensack, NJ; IISc Press, Bangalore, 2009.